JCB Article

Transmission of growth cone traction force through apCAM–cytoskeletal linkages is regulated by Src family tyrosine kinase activity

Daniel M. Suter and Paul Forscher

Department of Molecular, Cellular, and Developmental Biology, Yale University, New Haven, CT 06520

Tyrosine kinase activity is known to be important in neuronal growth cone guidance. However, underlying cellular mechanisms are largely unclear. Here, we report how Src family tyrosine kinase activity controls apCAM-mediated growth cone steering by regulating the transmission of traction forces through receptor–cytoskeletal linkages. Increased levels of tyrosine phosphorylation were detected at sites where beads coated with apCAM ligands were physically restrained to induce growth cone steering, but not at unrestrained bead binding sites. Interestingly, the rate and level of phosphotyrosine buildup near restrained beads were decreased by the myosin inhibitor 2,3-butanedione-2-monoxime, suggesting that tension promotes tyrosine kinase activation. While not affecting retrograde F-actin flow rates, genistein and the Src family selective tyrosine kinase inhibitors PP1 and PP2 strongly reduced the growth cone's ability to apply traction forces through apCAM–cytoskeletal linkages, assessed using the restrained bead interaction assay. Furthermore, increased levels of an activated Src family kinase were detected at restrained bead sites during growth cone steering events. Our results suggest a mechanism by which growth cones select pathways by sampling both the molecular nature of the substrate and its ability to withstand the application of traction forces.

Introduction

The neuronal growth cone integrates multiple tasks during axon guidance. It acts as a sensor, motility, and signal transduction device and each of these functions requires distinct molecular components. Axon guidance molecules can be segregated into long- or short-range cues, being attractive or repulsive (for reviews see Goodman, 1996; Tessier-Lavigne and Goodman, 1996). Furthermore, it is well known that significant reorganization of both the F-actin and microtubule cytoskeleton occurs during growth cone guidance events (for review see Tanaka and Sabry, 1995). A major challenge of growth cone research is now the dissection of the mechanisms and signaling pathways by which guidance receptors affect the dynamics and organization of the cytoskeleton that culminate in directed axonal growth.

Actin filaments are permanently turned over in the peripheral domain of growth cones, since they are assembled at the leading lamellar edge and tips of filopodia, undergo retrograde flow powered by myosin motors, and are finally recycled into actin monomers or short filaments (Forscher and Smith, 1988; Lin et al., 1996; Mallavarapu and Mitchison, 1999). Demonstration of an inverse relationship between retrograde F-actin flow and growth cone advance rates provided evidence for a model where substrate–cytoskeletal coupling regulates growth cone motility (Mitchison and Kirschner, 1988; Lin et al., 1994; Lin and Forscher, 1995). According to this model, cell surface receptors conditionally link extracellular substrates to retrograde moving F-actin networks and transduce flow into tension to direct forward growth cone movement, provided that the substrate is not too compliant. Direct support for growth cone steering by such a mechanism arose from our previous study on apCAM (Suter et al., 1998), the *Aplysia* homologue of vertebrate neural cell adhesion molecule (NCAM)* and member of the Ig superfamily of CAMs (Mayford et al., 1992; Walsh and Doherty, 1997). When beads coated with apCAM ligands

The online version of this article contains supplemental material.

Address correspondence to Dr. Paul Forscher, Department of Molecular, Cellular, and Developmental Biology, Yale University, P.O. Box 208103, New Haven, CT 06520-8103. Tel.: (203) 432-6344. Fax: (203) 432-6161. E-mail: paul.forscher@yale.edu

Key words: apCAM; Src family tyrosine kinase; tyrosine phosphorylation; receptor–cytoskeletal coupling; growth cone steering

*Abbreviations used in this paper: BDM, 2,3-butanedione-2-monoxime; CAM, cell adhesion molecule; CNS, central nervous system; Con A, Concanavalin A; DIC, differential interference contrast; PY, phosphotyrosine; PTK, protein tyrosine kinase; RBI, restrained bead interaction.

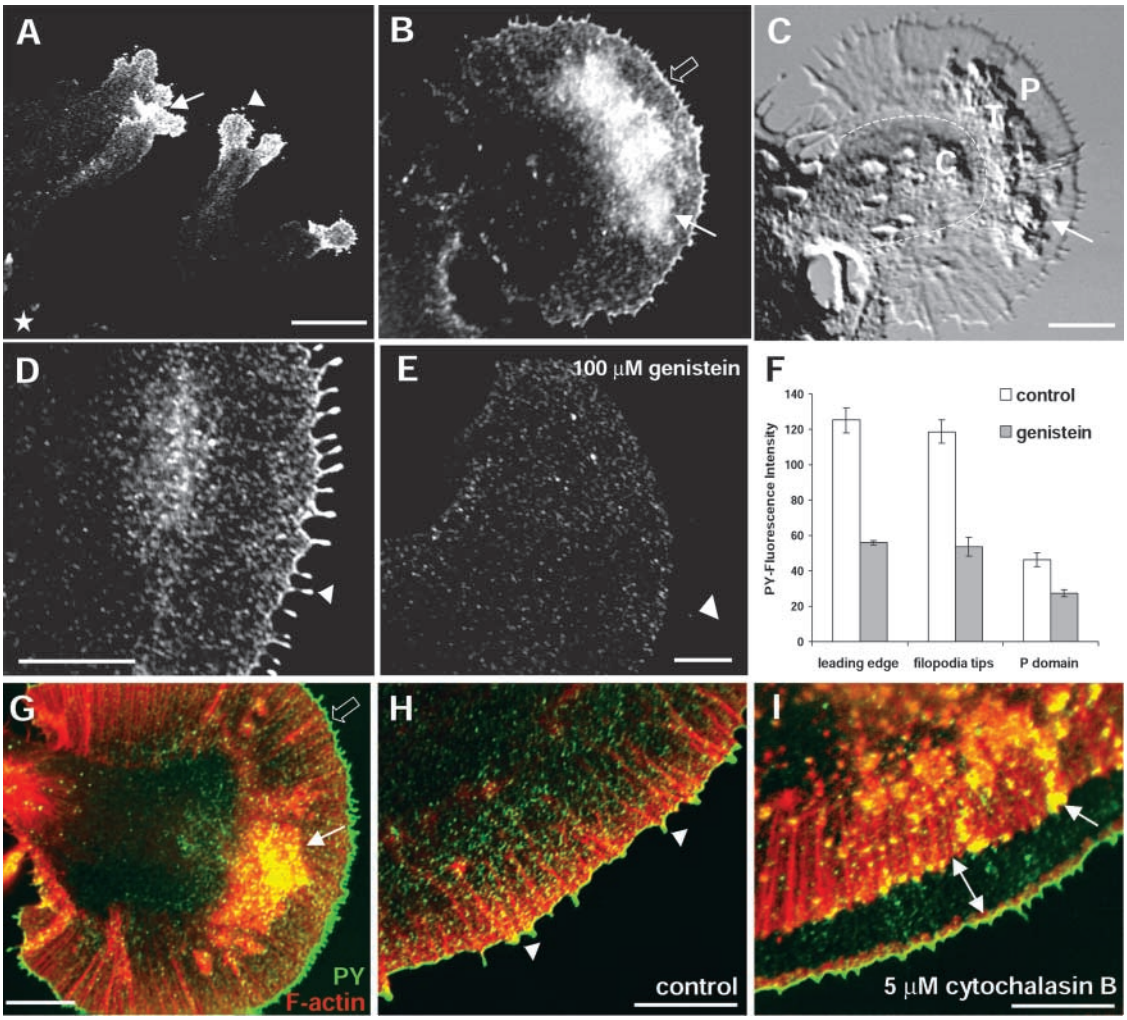

Figure 1. **Intense PY labeling at the leading edge, tips of filopodia, and in ruffles of growth cones.** PY immunocytochemistry using the 4G10 antibody in *Aplysia* growth cones. (A) Low power magnification view of bag cell neuron; cell body position is marked by star and arrow points to increased labeling at contact site. (B–E and G–I) High power magnification views of growth cones. (B and C) Same growth cone is shown with PY labeling (B) and in DIC optics (C). Peripheral domain (P), transition zone (T), and central domain (C) are indicated. Intense PY labeling was detected along the leading edge (open arrows; 170% increase in PY intensity compared with the peripheral domain, see F), at tips of filopodia (arrowheads; 155% increase), and in ruffles (arrows). (E) PY levels are reduced in growth cones treated with 100 μM genistein for 25 min. (F) Quantification revealed that genistein treatment decreased PY intensity at the leading edge by 55.4% ($P < 0.001$; *t* test), at filopodia tips (arrowhead in E) by 54.8% ($P < 0.001$), and in the peripheral domain by 41.7% ($P < 0.01$). Data represents average fluorescence intensity values ± SEM; $n = 7$ (control, 46 growth cones); $n = 3$ (genistein, 36 growth cones). (G–I) PY proteins (green) partially colocalize with F-actin structures (red) in ruffles (arrow in G), filopodia (arrowheads in H), and hot spots after cytochalasin B treatment (arrow in I). Treatment with 5 μM cytochalasin B for 1 min results in opening of an F-actin–free gap (double-headed arrow) that has reduced levels of PY proteins. Bars: (A) 50 μm; (B–E and G–I) 10 μm.

were placed on *Aplysia* growth cones and physically restrained against retrograde F-actin flow (restrained bead interaction [RBI]), structural and cytoskeletal changes such as flow attenuation and tension increase in the RBI axis were observed, very similar to growth cone interactions with cellular targets (Lin and Forscher, 1993, 1995; Suter et al., 1998). These findings, as well as a more recent study in mice on NrCAM (Faivre-Sarrailh et al., 1999), provided evidence that Ig CAMs can regulate growth cone guidance by acting as variable substrate–cytoskeletal coupling agents that transduce traction force (Suter and Forscher, 1998).

Both protein tyrosine kinases (PTKs) and phosphatases are involved in regulation of axon growth and guidance as revealed by both pharmacological and genetic studies (e.g., Williams et al., 1994; Orioli et al., 1996; Worley and Holt, 1996; Desai et al., 1997; Menon and Zinn, 1998; Wills et al., 1999). PTKs of the Src family (Maness et al., 1988; Helmke and Pfenninger, 1995) and tyrosine-phosphorylated proteins (Wu and Goldberg, 1993) have been localized in growth cones. Specifically, in the case of neurite growth mediated by the Ig CAMs, NCAM and L1, activation of both fibroblast growth factor receptor and nonreceptor PTKs of the Src family have been implicated in the signal transduction cascade (Beggs et al., 1994; Ignelzi et al., 1994; Doherty and Walsh, 1996; Maness et al., 1996; Saffell et al., 1997; Cavallaro et al., 2001). However, how CAM-induced phosphotyrosine (PY) signaling events regulate the receptor–cytoskeleton interactions and cytoskeletal dynamics that ultimately determine the direction and rate of growth cone movement is poorly understood.

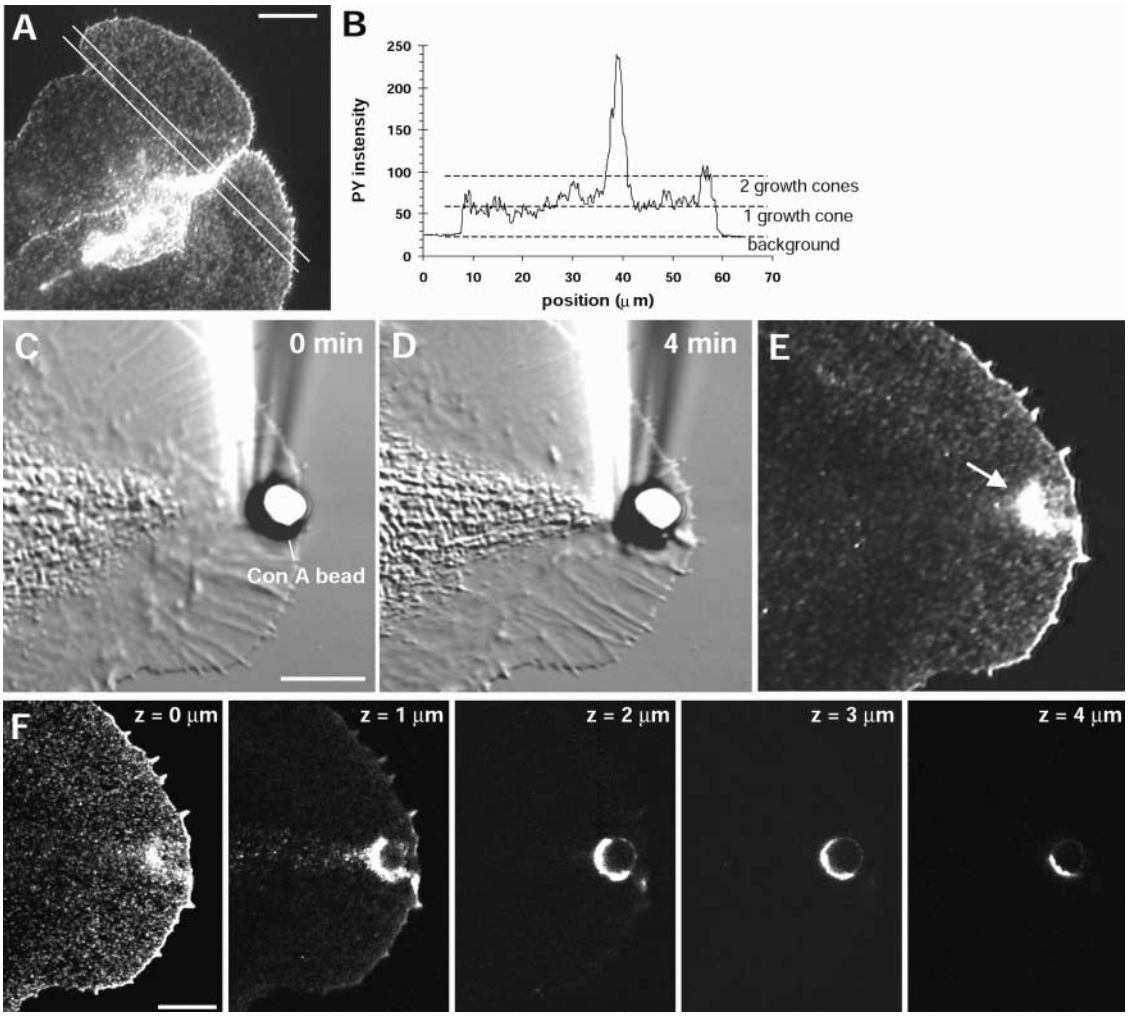

Figure 2. **Concentration of PY labeling at growth cone–growth cone contact sites and at Con A RBI sites.** (A) Increased PY labeling at growth cone–growth cone contact sites. Double lines indicate corridor through which average fluorescence intensity has been measured. (B) Plot of relative PY fluorescence intensity through the contact site indicated in A. (C and D) DIC images at start (C) and end (D, 4 min after start) of the central domain extension phase during a Con A RBI. (E and F) Conventional (E) and confocal fluorescence microscopy (F) reveal concentration of PY labeling around the bead (arrow). Confocal z-sections in 1-μm steps suggest that the growth cone membrane wraps around the bead. Generally, PY labeling was more intense at interaction sites using Con A beads when compared with apCAM beads: average PY accumulation factor of 7.0 ± 0.3 for Con A versus 4.1 ± 0.7 for apCAM beads, respectively. $n = 3$, $P < 0.01$. See also Video 1, available at http://www.jcb.org/cgi/content/full/jcb.200107063/DC1. Bars, 10 μm.

In this report, we address this issue and show that tyrosine kinase activity regulates apCAM–cytoskeletal coupling and transmission of traction forces during growth cone steering events. Increased PY labeling was detected at apCAM–actin junctions where tension is transduced. We provide evidence that Src family tyrosine kinase activity is necessary for the strengthening of apCAM–F-actin linkages that leads to the generation of traction force. Interestingly, we found that tension in receptor–F-actin linkages is a prerequisite for tyrosine phosphorylation, suggesting positive feedback between tension and PTK activation.

Results

PY distribution in growth cones

We first analyzed the PY distribution in *Aplysia* bag cell growth cones cultured on polylysine substrate in the absence of any immobilized apCAM ligands (Fig. 1). The majority of the growth cones (79 ± 3%) exhibited enrichment of PY labeling relative to the proximal neurite (Fig. 1 A; $n = 11$, 250 growth cones). The punctate PY labeling was more intense in the peripheral domain and transition zone than in the central domain (Fig. 1, B and C). Intense PY signals were detected along the leading edge (Fig. 1, B and G, open arrows), at tips of filopodia (Fig. 1, A and D, arrowheads), and within ruffles in the transition zone (Fig. 1 B, C and G, arrows). The concentration of PY proteins in filopodia tips is in agreement with an earlier report (Wu and Goldberg, 1993). Growth cones treated with 100 μM genistein, a widely used broad-spectrum PTK inhibitor, had a significant decrease of PY labeling when compared with controls (Fig. 1, E and F).

Since the leading edge, tips of filopodia, and ruffles are specialized sites of F-actin assembly (Forscher and Smith, 1988; Mallavarapu and Mitchison, 1999; Rochlin et al., 1999), we investigated the respective distribution of F-actin

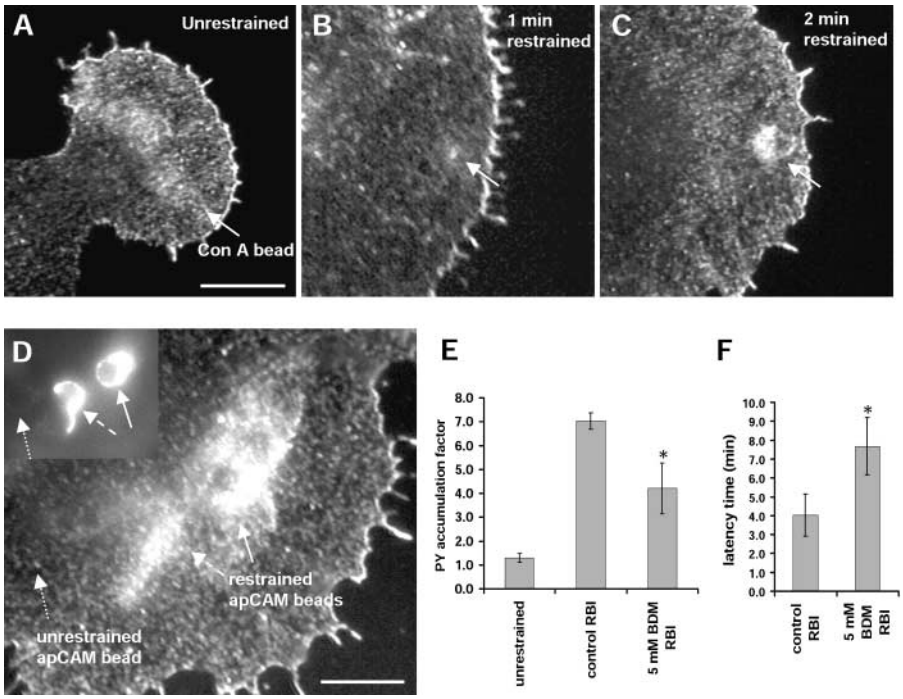

Figure 3. **Correlation between tension and PY build up.** (A–D) PY build up with increasing restraining time. (A–C) Con A beads were either unrestrained and moved with retrograde flow for 1 min (A) or restrained for the times indicated before RBI was completed (B and C, arrows point to bead positions). We used Con A beads in these experiments since their RBI latency times are less variable and generally shorter than those observed using apCAM beads (Suter et al., 1998). PY labeling at bead sites increased by 25% after 1 min of restraint (B) and by 90% after 2 min of restraint (C). (D) apCAM beads were either unrestrained (dotted arrow) or restrained for 1 (dashed arrow) or 2 min (solid arrow). Inset shows higher focus level to illustrate PY labeling around restrained beads. (E and F) BDM decreases PY buildup and increases RBI latency times. (E) Quantification of PY intensity at unrestrained Con A beads as well at Con A RBI sites. PY protein levels near restrained Con A beads were reduced in 5 mM BDM compared with control interactions. Asterisk indicates $P < 0.05$, *t* test, $n = 3$ (unrestrained); $n = 3$ (control RBI); $n = 4$ (BDM RBI). (F) Latency times of Con A RBIs under control conditions ($n = 6$) and in 5 mM BDM ($n = 4$, asterisk indicates $P < 0.05$). Bars, 10 μm.

structures and PY proteins (Fig. 1, G–I). Bundles of actin filaments span the width of the lamellipodia and terminate at the leading edge or within filopodia, where they partially overlap with PY proteins (Fig. 1, G and H). In addition, patches of PY labeling colocalized with F-actin–containing ruffles (Fig. 1 G, arrow). Furthermore, we investigated the localization of PY proteins in growth cones treated for 1 min with 5 μM cytochalasin B to block plus-end F-actin assembly (Fig. 1 I). This treatment results in a band devoid of F-actin structures that widens over time as filament networks are withdrawn by the continuing process of retrograde flow (Forscher and Smith, 1988). The average PY intensity in the F-actin–free zone was reduced by 39 ± 5% compared with adjacent peripheral domain regions ($n = 13$ growth cones), suggesting that a significant number of PY proteins are cycling with the actin filaments that maintain retrograde flow. Interestingly, a narrow band of cytochalasin-resistant F-actin remained in place at the leading edge together with strong PY labeling (Fig. 1 I). These data, together with genistein effects on growth cone dynamics, suggest a role for tyrosine phosphorylation in the regulation of F-actin assembly (to be reported separately); this paper will focus on tyrosine kinase regulation of traction force generation through apCAM–cytoskeletal linkages during growth cone steering.

High levels of tyrosine phosphorylation at sites where apCAM transduces tension

To investigate a role for tyrosine phosphorylation in conditional apCAM–cytoskeletal coupling, we examined the distribution of PY proteins at sites where apCAM is believed to transduce actomyosin-based tension (Figs. 2 and 3). Enrichment of PY labeling was found at native growth cone–growth cone interaction sites (Figs. 1 A and 2 A). Quantification revealed that the PY signal in the region of growth cone contact was about five times higher than in adjacent peripheral domains (Fig. 2 B). Note that a similar accumulation of apCAM at native growth cone interaction sites has been reported previously (Thompson et al., 1996; Suter et al., 1998).

Increased PY labeling was also detected at sites where beads coated with apCAM ligands, such as Concanavalin A (Con A) or apCAM protein, were physically restrained using the RBI assay to induce growth cone steering events that involve tension transduction (Fig. 2, C–F, see also Video 1, available at http://www.jcb.org/cgi/content/full/jcb.200107063/DC1; Suter et al., 1998). Con A, a lectin that binds apCAM, among other *Aplysia* membrane proteins, is a potent RBI-inducing agent (Thompson et al., 1996; Suter et al., 1998). The topology of PY enrichment at RBI sites was investigated by taking z-sections with a confocal microscope, revealing that PY proteins concentrate near, and wrap around the bead surface over a range of at least 3 μm in z-axis (Fig. 2 F). The confocal data also demonstrate that the intense PY labeling at bead interaction sites is not due to a thickness artifact. An increase in PY labeling was also detected at RBI sites using beads coated with apCAM protein, when such beads were transiently restrained (before RBI completion; Fig. 3 D), or after completed RBIs (unpublished data). To summarize, increased levels of tyrosine phosphorylation appeared to be focused at sites of tension transduction through substrate–cytoskeletal linkages.

Tension is necessary for tyrosine phosphorylation

To further investigate the relationship between tyrosine kinase activation and tension, we restrained Con A beads for varying amounts of time and then assessed PY levels (Fig. 3, A–C). Interestingly, unrestrained Con A beads did not elicit perceptible changes in PY labeling at bead contact sites (Fig. 3 A).

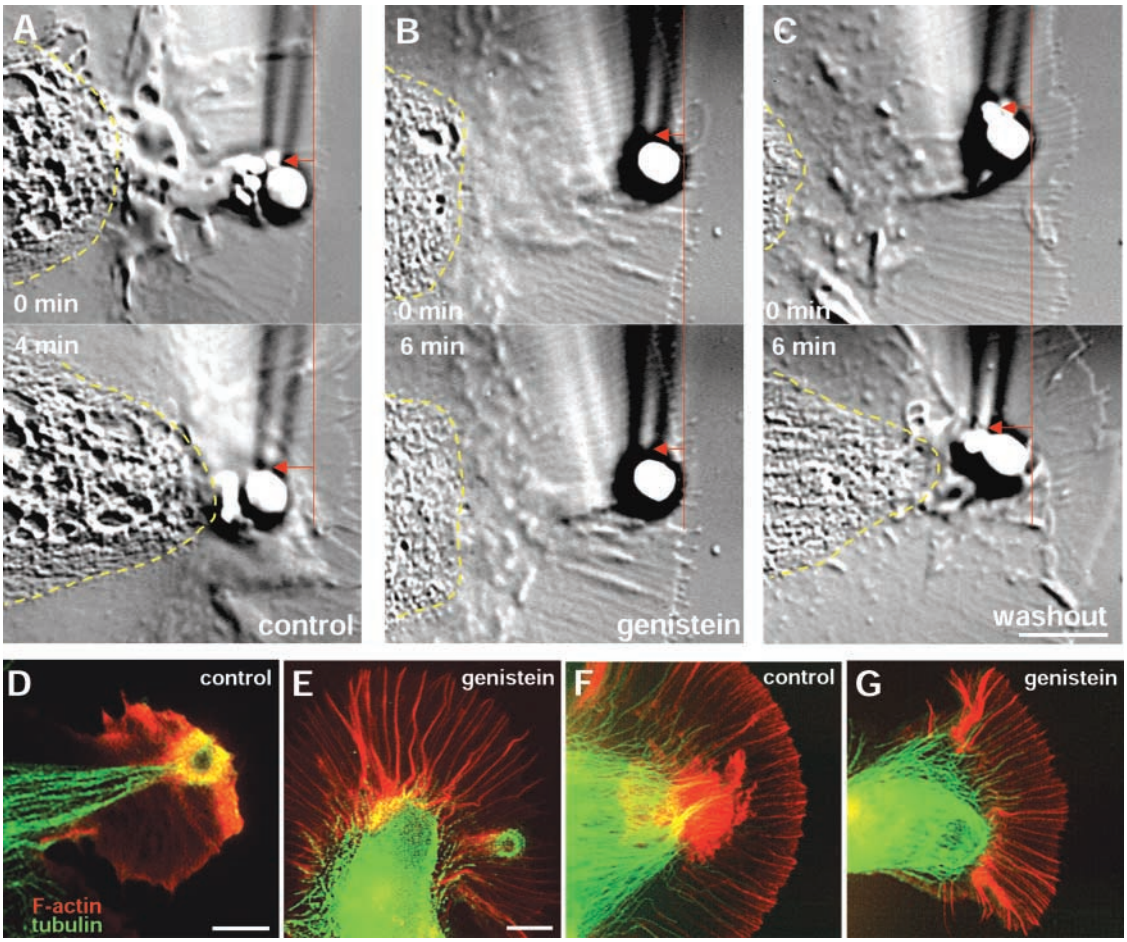

Figure 4. **Tyrosine kinase inhibition uncouples apCAM-mediated RBIs.** (A–C) ApCAM RBI capability using 4E8 beads was tested on the same growth cone shown in control (A; 0.5% DMSO), after treatment with 100 μM genistein for 20 min (B), and after drug washout (C; 0.5% DMSO). Top, growth cone at the start of central domain extension (boundary marked by dashed yellow line) or, in the case of genistein, when central domain extension would have been expected. Bottom, completed RBI when central domain reached the bead or, in the case of the genistein, after a total restraining time of 16 min, which accounts for more than average control latency plus interaction times. RBI fully recovered after drug washout (C). (D and E) Cytoskeletal reorganizations typical of control RBIs (D) are absent after treatment with 100 μM genistein (E). Green signal around bead in E (yellow in D because of F-actin accumulation in control RBIs) results from the detection of the 4E8 antibody on the bead by the secondary antibody used for tubulin immunofluorescence. (F and G) F-actin and microtubule distribution in controls (F) and growth cones treated with 100 μM genistein for 25 min (G) without any bead interactions. Bars, 10 μm.

However, restraining Con A beads for 1 min, a period too brief to promote an RBI, resulted in detectable increases in PY labeling (Fig. 3 B, arrow). When beads were restrained for 2 min, PY labeling further intensified, again, before an RBI was completed (Fig. 3 C). After Con A RBI completion, PY levels at interaction sites were ~6–7 times higher than levels measured in the adjacent peripheral domain or around unrestrained beads (Fig. 3 E). A similar correlation was observed with apCAM beads: unrestrained beads did not alter baseline levels of PY labeling, whereas restrained beads augmented their PY labeling as a function of restraining time (Fig. 3 D).

The correlation between bead restraint and PY buildup suggested that tension might promote tyrosine phosphorylation. To further test this, we pretreated the neurons for 10 min with 5 mM of the myosin ATPase inhibitor 2,3-butanedione-2-monoxime (BDM). This dose of BDM attenuates retrograde F-actin flow rates by ~30%, but does not block RBI completion (unpublished data; Lin et al., 1996). BDM treatment resulted in a significant 40% decrease of PY labeling at Con A RBI sites relative to control RBIs (Fig. 3 E). Reduced PY labeling was accompanied by a 93% increase in interaction latency times (Fig. 3 F). These observations suggest that actomyosin-based tension is required for activation of the tyrosine kinase(s) involved.

Src family tyrosine kinase activity regulates apCAM–cytoskeletal coupling in RBIs

To investigate if PTK activity is required for apCAM–cytoskeletal coupling and tension transduction, we looked at the effects of PTK inhibition. We first assessed actions of genistein on RBIs using beads coated with the apCAM antibody 4E8 (Fig. 4). In control interactions, central domain extension was accompanied by leading edge growth distal to the bead as well as by progressive needle bending (red arrows from red marker line), demonstrating that the growth cone builds up tension and exerts a pulling force on the bead substrate (Fig. 4 A). All of these typical RBI characteristics were absent in the same growth cone after treatment with 100

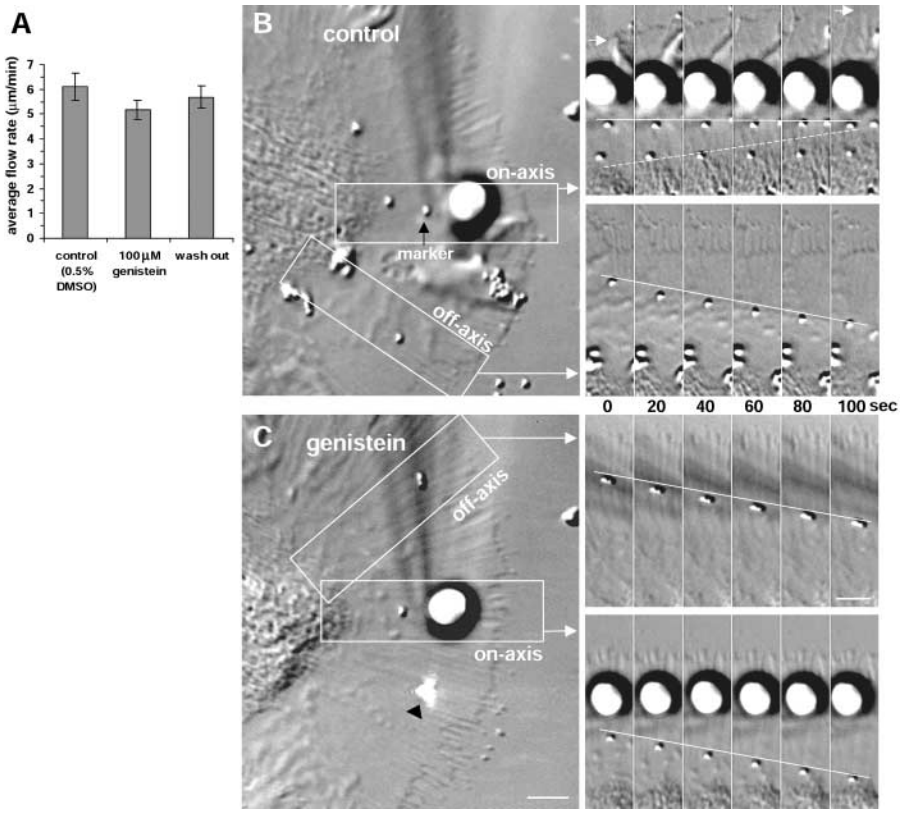

Figure 5. **PTK inhibition uncouples RBIs without affecting retrograde F-actin flow.** (A) Quantification of retrograde F-actin flow effects by treatment with 100 μM genistein for 25 min on growth cones without RBIs. Average values ± SEM for control ($n = 6$), drug ($n = 6$), and wash out ($n = 3$) flow rates are: 6.11 ± 0.56, 5.18 ± 0.56, 5.69 ± 0.46 μm/min, respectively; $P > 0.1$; 50–90 beads analyzed per condition. (B and C) PTK inhibition does not affect flow during uncoupled RBIs. All images refer to the same growth cone. Flow marker beads were placed with a laser tweezer both within the interaction corridor (on-axis) and on adjacent areas (off-axis) during an 4E8 RBI under control conditions (B) and after pretreatment with 50 μM genistein for 20 min (C). Panels on the right show simultaneous DIC time sequences of on- and off-axis bead movements in areas of interests marked on the left. Flow rates for the displayed on- and off-axis beads are 0.31 versus 5.64 μm/min in control and 4.47 versus 5.14 μm/min in genistein. Central domain extension in control is indicated by dashed line and leading edge growth by a white arrow. Laser beam focus is marked with an arrowhead in C. Bars, 5 μm.

μM genistein for 20 min (Fig. 4 B) and fully recovered after drug washout (Fig. 4 C). Cytoskeletal rearrangements typical of control RBIs, such as F-actin accumulation around and microtubule extension toward the bead, were not observed in genistein (Fig. 4, D vs. E). Besides inhibition of apCAM-mediated RBIs, genistein caused filopodial elongation as reported earlier (Wu and Goldberg, 1993), and reduction of transition zone ruffling activity (compare Fig. 4, A and B). The general distribution of F-actin bundles and microtubules of control growth cones without RBIs was not significantly affected by genistein (Fig. 4, F vs. G).

To test if RBI inhibition by genistein resulted from an effect on retrograde F-actin flow, we measured flow rates using a laser trap–assisted bead assay (Lin and Forscher, 1995). Retrograde F-actin flow was not significantly different from controls after 25 min in 100 μM genistein and did not change after genistein removal (Fig. 5 A). We then analyzed flow rates in the RBI axis in the absence or presence of the inhibitor (Fig. 5, B and C). During a normal RBI, retrograde flow along the RBI axis is strongly attenuated relative to off-axis flow rates (Fig. 5 B): 0.65 ± 0.29 versus 5.81 ± 0.11 μm/min; $n = 3$, $P < 0.0001$. In contrast, on- and off-axis beads moved at similar rates in the presence of 50 μM genistein (Fig. 5 C): 4.90 ± 0.51 versus and 5.29 ± 0.64 μm/min; $n = 3$, $P > 0.1$.These results indicate that PTK inhibition resulted in "slippage" between apCAM molecules and underlying moving F-actin networks.

We found that RBIs were sensitive to herbimycin A (Fig. 7), a relatively selective Src family PTK inhibitor; therefore, we further investigated a role for this group of nonreceptor PTKs in apCAM–cytoskeletal coupling with two other selective inhibitors, PP1 and PP2. Treatment of growth cones with 10 μM PP1 for 20 min had very little effect on growth cone morphology, dynamics, and cytoskeletal distributions (Fig. 6, A–D). We observed slight filopodia elongation in some growth cones (Fig. 6, A and B, arrows), but never to the extent found with 100 μM genistein. Transition zone ruffling activity was not reduced by PP1 (Fig. 6, A and B) and retrograde flow was not affected (unpublished data). Thus, treatment with 10–25 μM PP1 had minimal effects on growth cone morphology and dynamics; in contrast, this agent had strong inhibitory effects on apCAM-mediated growth cone steering (Fig. 6, E–G, see also Videos 2–4, available at http://www.jcb.org/cgi/content/full/jcb.200107063/DC1). Typical control RBI attributes, such as central domain extension and reorientation toward the restrained bead (Fig. 6 E), were completely absent in the presence of PP1 (Fig. 6 F) and recovered after drug removal (Fig. 6 G).

Quantification of apCAM RBI uncoupling by PP1 and other PTK inhibitors is shown in Fig. 7. For each inhibitor experiment, RBI capability of a particular growth cone was first tested under control conditions. RBI probability was reduced by PP1, PP2, and genistein in a dose-dependent manner and effects were almost completely reversible. RBIs were not affected by the corresponding inactive structural analogues PP3 (control for PP1 and PP2) and daidzein (control for genistein). PP2, which had minimal effects on growth cone morphology and dynamics as PP1 (Fig. 9, D and E), appeared somewhat more potent in RBI inhibition relative to PP1. Latency times of RBIs that were completed in the presence of a PTK inhibitor were increased compared with controls. For example, the average latency time in 10 μM PP1 was increased by 88% ($n = 6$;

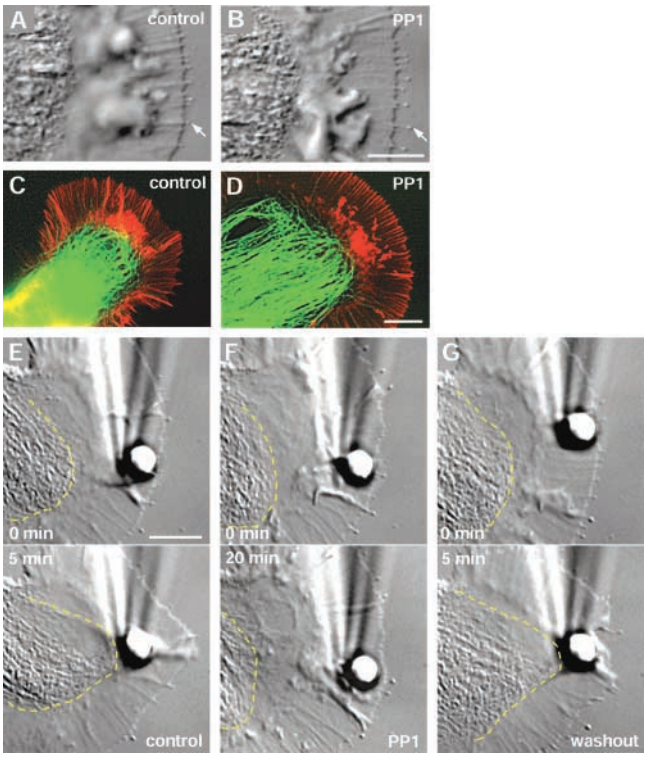

Figure 6. **The Src family selective PTK inhibitor PP1 uncouples apCAM-mediated RBIs.** (A–D) PP1 has minimal effects on growth cone morphology and cytoskeletal distribution. (A and B) High power magnification DIC images of the same growth cone in control condition (A) and after 20 min treatment with 10 μM PP1 (B). Note, no effect on ruffling and very little effect on filopodia extension (arrows). (C and D) F-actin and microtubule organization in control condition (C) and in 10 μM PP1 (D). (E) RBI with a 4E8-coated bead in control condition at start (top) and when the central domain reached the bead (bottom; boundary marked with yellow line). (F) The same growth cone after treatment with 25 μM PP1 for 20 min did not respond to the restrained apCAM substrate, even after a total restraining time of 30 min (G) RBI capability of this growth cone was recovered after drug washout. See also Videos 2–4, available at http://www.jcb.org/cgi/content/full/jcb.200107063/DC1. Bars, 10 μm.

$P < 0.001$). Finally, it should be noted that PTK inhibition weakens but does not totally disrupt apCAM-actin network linkages, placing growth cones in a state where they cannot develop significant traction force with respect to restrained beads. Evidence for this comes from observing beads in the presence of PTK inhibitors after needle restraint was removed. In this case, beads immediately move in the retrograde direction, indicating some level of actin coupling; however, the linkage clearly was not strong enough to support a typical RBI response (see Video 3, available at http://www.jcb.org/cgi/content/full/jcb.200107063/DC1). These results provide evidence that Src family PTK activity is necessary for strong apCAM–cytoskeletal coupling and subsequent force generation during growth cone steering events.

Increased levels of activated Src family PTK at RBI sites

To further substantiate a role for an Src family kinase, we used a phosphospecific antibody that recognizes the autophosphorylation site PY418 of activated Src family PTKs, a

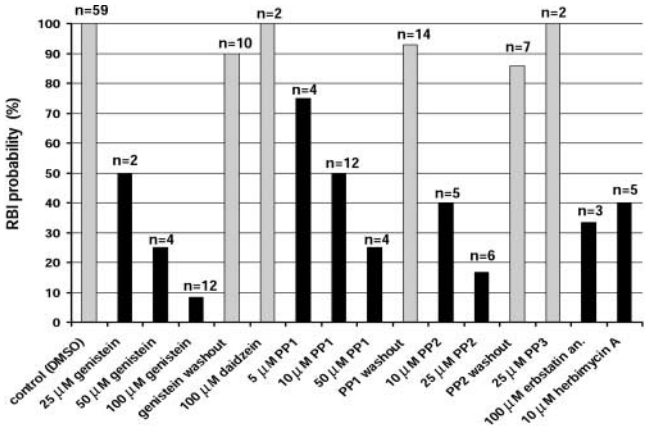

Figure 7. **Quantification of RBI inhibition by PTK inhibitors.** RBI probability is indicated as the percentage of successfully completed RBIs per total number of experiments (n). PTK inhibitor experiments are shown as black bars, control RBIs as gray bars. Only PTK inhibitor RBI experiments that were preceded with a successfully completed control RBI on the same growth cone were taken into these statistics.

sequence highly conserved among different members of this family and across species (Sicheri and Kuriyan, 1997; Thomas and Brugge, 1997). In Western blots of *Aplysia* central nervous system (CNS) extracts prepared in the presence of tyrosine phosphatase inhibitors, this antibody (Src PY418) recognized a single band at 60 kD, consistent with an Src family PTK (Fig. 8 A, lane 1). In the presence of PP1, the intensity of this band was reduced (lane 2). As a further control for the phosphospecific antibody, the band was strongly reduced in samples where tyrosine phosphatase inhibitors were omitted (lane 3). As a positive control, the antibody recognized a band at 60 kD in a cell lysate from chicken embryonic fibroblasts expressing Src (lane 4).

Immunolocalization with this antibody in *Aplysia* growth cones revealed a relatively equal distribution of puncta throughout the growth cone as well as along the length and tips of filopodia (arrow and arrowhead in Fig. 8 B). Imaging thicker regions, such as branching neurites, suggested that Src PY418 puncta are localized close to the plasma membrane (Fig. 8 C). As expected, double labeling with the PY antibody 4G10 revealed colocalization only in a small subpopulation of puncta and, interestingly, little Src PY418 labeling along the PY-rich leading edge (Fig. 8 D).

We then examined Src PY418 labeling at 4E8 bead RBI sites and found increased levels at restrained bead binding sites (Fig. 9, A–C). We detected on average 2.3 ± 0.5 times as much activated Src PY418 labeling accumulated around restrained beads relative to adjacent peripheral domain areas ($n = 4$). In contrast, unrestrained beads (Fig. 9 C, arrow) had insignificant labeling with an accumulation factor of 1.2 ± 0.2, comparable to background levels of beads not touching the cell (arrowhead; $n = 4$, $P > 0.1$). Fig. 9, D–F shows an RBI which was blocked by 25 μM PP2 and subsequently labeled for Src PY418. The average Src PY418 accumulation factor for PP2 blocked RBI sites was 1.2 ± 0.2, i.e., similar to background levels ($n = 3$, $P > 0.1$). Together, these data further support a role for Src family PTK activity in the regulation of apCAM–cytoskeletal coupling and force transduction during growth cone steering.

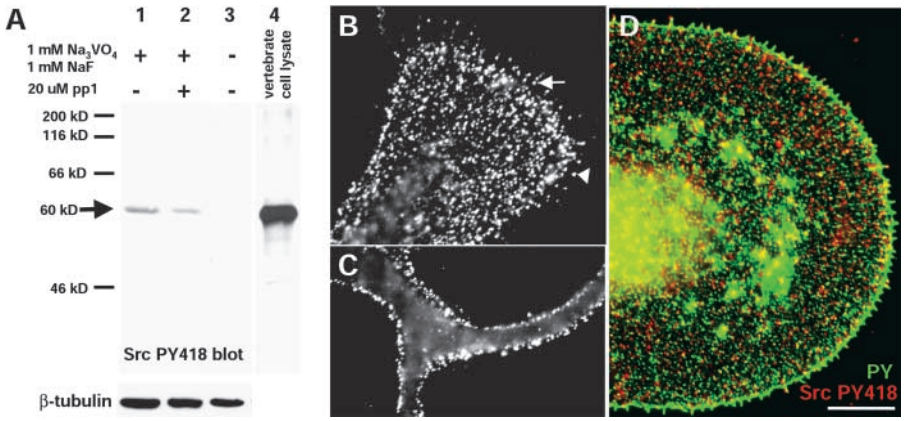

Figure 8. **Immunolocalization of an activated Src family PTK in growth cones.** (A) Western blot characterization of Src PY418 antibody using *Aplysia* CNS proteins extracted under different tyrosine kinase and phosphatase inhibitor conditions as indicated and separated on a 10% SDS-PAGE. A control lysate from chicken embryonic fibroblasts was loaded in lane 4. Reprobing for β-tubulin was done to normalize for equal protein loading. The 60-kD band in *Aplysia* CNS extracts was reduced by 41% using 20 μM PP1 in the experiment shown (lane 2). An average reduction of 71 ± 3% was found using 50 μM PP1 ($n = 2$). Molecular weights are indicated. (B–D) Immunocytochemistry of growth cones (B and D) and branching neurites (C) in culture using the Src PY418 antibody. (D) Double-staining for total PY (green) and activated Src family PTK (red). Bar, 10 μm.

Discussion

It is well known that tyrosine phosphorylation is important in signal transduction pathways downstream of cell surface receptors mediating growth cone guidance. However, the functional consequences of tyrosine phosphorylation on underlying CAM–cytoskeleton interactions and cytoskeletal dynamics are poorly understood. In the present study, we provide evidence that tyrosine phosphorylation and Src family PTK activity are necessary for strengthening of apCAM–F-actin linkages that are required for tension generation during growth cone steering events.

Src family tyrosine kinase activity regulates apCAM–cytoskeletal coupling

For growth cone filopodia, several potential roles for tyrosine phosphorylation have been proposed, including regulation of actin-dependent filopodia dynamics, receptor localization, and receptor–actin linkages (Goldberg and Wu, 1996). Our results focusing on growth cone lamellipodia strongly suggest that tyrosine phosphorylation can control growth cone motility and guidance by regulating CAM–cytoskeletal coupling and thereby tension generation (Mitchison and Kirschner, 1988; Lin et al., 1994; Suter and Forscher, 1998). Intensified PY labeling was found at sites where apCAM transduces actomyosin-based tension. PY buildup increased with restraining time during the latency phase of RBIs; however, use of unrestrained beads revealed that apCAM clustering alone was not sufficient to elicit increased tyrosine phosphorylation.

RBIs were blocked by PTK inhibitors, including the broad spectrum agent, genistein (Akiyama et al., 1987), and the Src family selective inhibitors PP1 and PP2 (Hanke et al., 1996), suggesting that Src family tyrosine kinase activity is necessary for strong apCAM–cytoskeletal coupling and subsequent growth cone steering effects, including tension generation and directed central domain and microtubule extension. We believe the inhibitor effects are specific, since they are dose-dependent, reversible, and not observed with corresponding control drugs daidzein and PP3. The doses of PP1 and PP2 used in our *Aplysia* studies are in the range used for Src family PTK inhibition in vertebrate cells and tissues (Sanna et al., 2000; Mohamed et al., 2001). We were able to establish conditions for PP1 and PP2 whereby the drugs had minimal effects on growth cone morphology, cytoskeletal distribution, or retrograde F-actin flow, yet had robust inhibitory effects on growth cone steering. It follows that PTK inhibition of RBI activity is likely due to perturbation of apCAM–cytoskeletal linkages, rather than disruption of cytoskeletal structures. In addition, the prolonged absence of tension build up and continued presence of F-actin flow in the RBI axis during PTK inhibition provides evidence that "slippage" in these linkages is possible and can be modulated by tyrosine phosphorylation. We speculate that slippage after PTK inhibition is similar to that normally observed during the RBI latency phase, where target beads are only weakly coupled to retrograde flow (Suter et al., 1998). Further evidence for an Src family PTK role in tension generation through apCAM–actin linkages comes from our studies with the Src PY418 antibody, where labeling accumulated around restrained beads in the absence, but not in the presence, of PP2. Together, these observations suggest that tension development in our growth cone steering assay depends on strengthening of apCAM–actin linkages subsequent to Src family PTK activation near restrained beads.

The two major candidates for the kinase involved are Src itself and Fyn, since they are prominent Src family members found in growth cones (Maness et al., 1988; Helmke and Pfenninger, 1995; Burden-Gulley and Lemmon, 1996), are associated with Ig CAM complexes (Kunz et al., 1996; Beggs et al., 1997), and are involved in Ig CAM-mediated neurite growth (Beggs et al., 1994; Ignelzi et al., 1994) and guidance (Morse et al., 1998). Our immunostaining for activated Src family PTK revealed a punctate distribution in *Aplysia* growth cones, similar to the localization of total Src and Fyn protein reported previously for retinal ganglion cell growth cones (Burden-Gulley and Lemmon, 1996). Since both PP1 and PP2 and the Src PY418 antibody do not distinguish between these two Src family PTKs, a goal for future work will be testing if either or both of the *Aplysia* homologues of these kinases regulate apCAM–actin filament coupling.

Our work also provides new insights regarding potential Src family PTK function in growth cones, an area not yet well characterized. Previous studies have shown that Src

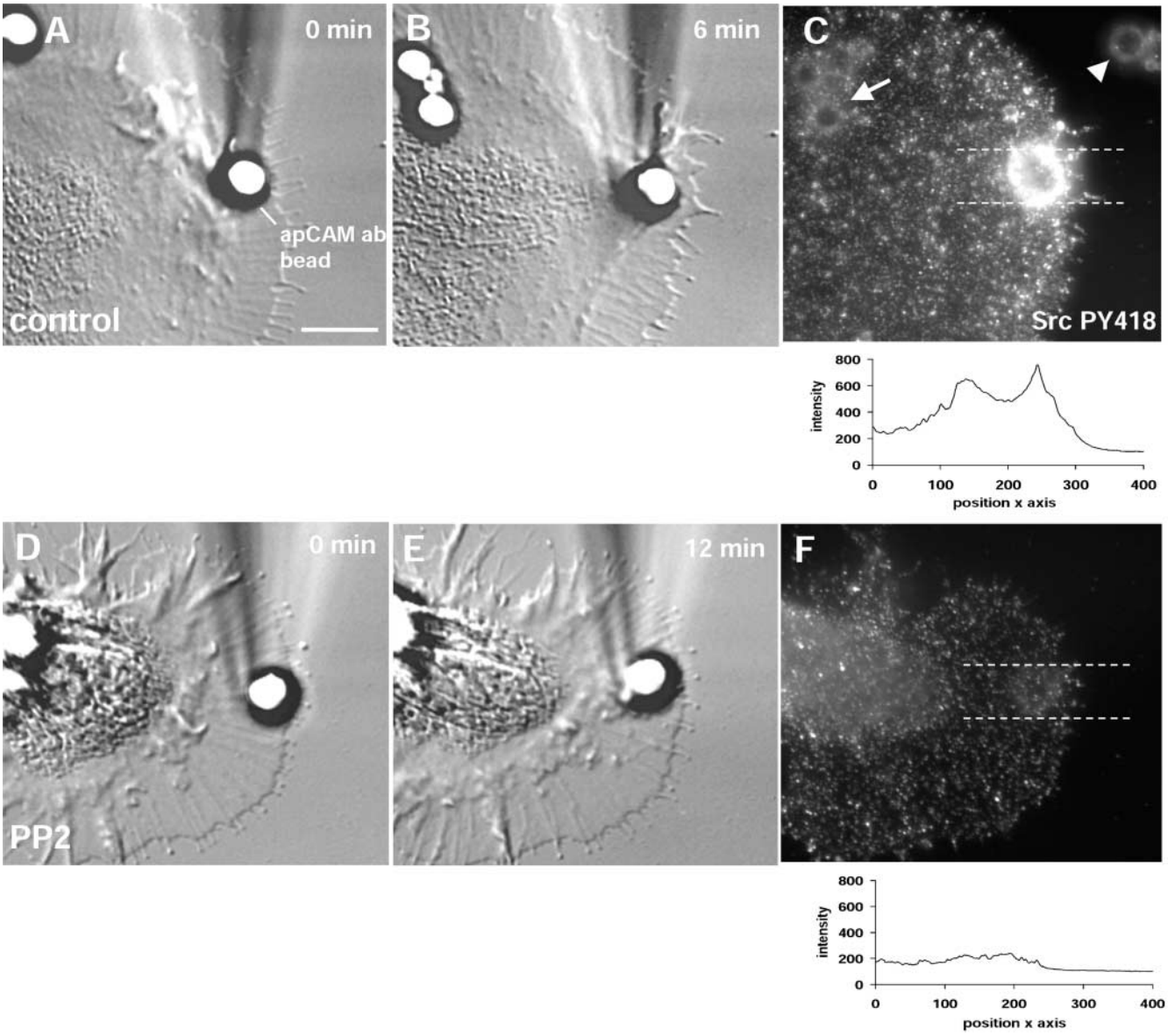

Figure 9. **Increased levels of activated Src family PTK at RBI sites.** (A–C) Control RBI with a 4E8 bead at start (A) and end (B) of interaction. (C) Increased Src PY418 signal at RBI site compared with unrestrained beads (arrow) or control beads on the substrate (arrowhead). Lower panel shows Src PY418 intensity line scan through interaction site indicated with dashed lines. (D–F) RBI experiment with a 4E8 bead which was blocked by 25 μM PP2 at start (D) and after 12 min of bead restraint (E). (F) The levels of activated Src family PTK labeling at bead site was reduced by 78% compared with the control condition shown in C. Bar, 10 μm.

phosphorylates α- and β-tubulin in growth cone membrane preparations (Matten et al., 1990) and addition of purified N-CAM and L1 reduced tyrosine phosphorylation of tubulin (Atashi et al., 1992). Therefore, it has been speculated that Ig CAMs could mediate neurite growth and guidance through regulation of microtubule dynamics by Src family PTKs (Atashi et al., 1992). We have not found any obvious effects of Src family PTK inhibition on microtubule distribution in growth cones; however, we cannot exclude a role for Src PTKs in the regulation of axonal microtubule and/or microtubule-associated protein function that could affect axonal growth properties. Finally, it should be kept in mind that Src's action may be complex given recent evidence that L1-mediated neurite outgrowth depends on Src-regulated, mitogen-activated protein kinase activation and endocytosis of L1 (Schaefer et al., 1999; Schmid et al., 2000).

An interesting area for further investigation will be the Src family PTK substrates in the apCAM–actin linkage complex. apCAM itself is not a likely candidate, since the only intracellular tyrosine residue is at the border of the membrane-spanning domain (Mayford et al., 1992). Information on the regulation of receptor–actin linkages by Src family PTKs has already emerged from studies on the integrins and focal adhesions in fibroblasts, where structural proteins (e.g., paxillin) as well as signaling proteins (e.g., FAK, $p130^{Cas}$) were found to be phosphorylated by Src (for reviews see Burridge and Chrzanowska-Wodnicka, 1996; Schoenwaelder and Burridge, 1999) and Src appears to regulate integrin

receptor–cytoskeletal interactions involved in fibroblast migration (Felsenfeld et al., 1999).

Tension promotes tyrosine phosphorylation

It is well established that growth cones exert pulling or traction forces and tend to advance in response to applied tension (Bray, 1984; Lamoureux et al., 1989). Here, we provide evidence for a correlation between tension development and tyrosine phosphorylation. First, unrestrained beads that cannot produce tensioning force did not exhibit increased PY levels; second, reducing contractility with a myosin ATPase inhibitor reduced PY labeling, rate of PY accumulation, and increased RBI latency times; third, tension buildup during RBIs was sensitive to PTK inhibitors. Together, these results suggest that tension promotes tyrosine phosphorylation, which is required for strengthening of apCAM–cytoskeletal linkages in order to generate the level of tension necessary for RBI completion. An intriguing question relates to the trigger for PTK activation: how does the combination of restraint and apCAM clustering lead to kinase activation? Relatively brief (~1 min) periods of restraint were enough to promote tyrosine phosphorylation near apCAM beads. If, during such brief periods, tension levels were indeed rising, they were not of sufficient magnitude to result in changes in retrograde flow or needle deflection. It will be of interest to examine the restraining force versus PTK activation relationship in detail using a more sensitive detector, such as a calibrated laser trap (Choquet et al., 1997; Felsenfeld et al., 1999).

Activation of tyrosine phosphorylation by tension and mechanical stress has also been reported for the integrins, an established family of mechanotransducers (Wang et al., 1993). Rho-dependent contractility promotes focal adhesion and stress fiber formation as well as tyrosine phosphorylation in fibroblasts (Chrzanowska-Wodnicka and Burridge, 1996). Mechanical stress applied to integrins using magnetic beads resulted in tyrosine phosphorylation of cytoskeleton-associated proteins (Glogauer et al., 1997; Schmidt et al., 1998), and the level of tyrosine phosphorylation in focal adhesions increases with the rigidity of the extracellular matrix (Pelham and Wang, 1997; Katz et al., 2000). Thus, fibroblasts are able to sense substrate rigidity and dynamically respond to applied forces by strengthening integrin–cytoskeletal linkages (Choquet et al., 1997; Riveline et al., 2001). Significantly, there appears to be an increasing consensus across different families of CAMs and different cellular systems for a positive feedback model: immobilized receptor–cytoskeletal linkages transmit forces that stimulate tyrosine phosphorylation and thereby linkage strengthening; this leads to further buildup of tension and tyrosine phosphorylation and so on. During a growth cone steering event involving apCAM, this cyclical process continues until the apCAM–actin linkage complex is stiff enough to generate traction forces sufficient for promoting axon growth and guidance. Such a mechanism may enable growth cones to sense not only the molecular nature of a potential substrate but also its compliance, responding most strongly to substrates capable of generating traction force, thereby facilitating migration down the path providing the best grip.

Materials and methods

Proteins, antibodies, and chemical reagents

Purification of apCAM from *Aplysia* CNS as well as of the monoclonal apCAM antibody 4E8 (Keller and Schacher, 1990; Mayford et al., 1992) was performed as reported (Suter et al., 1998). 4E8 hybridomas were kindly provided by the laboratory of E. Kandel (Columbia University, New York, NY). Biotinylated Con A and avidin D were from Vector Laboratories. The monoclonal PY antibody 4G10 was from Upstate Biotechnology and the phosphospecific rabbit anti-Src PY418 antibody was from Biosource International. This Src PY418 antibody recognizes the conserved autophosphorylation site of Src family PTKs, typically referred to as Y416 in chick (Sicheri and Kuriyan, 1997; the name of the antibody is based on a specific chick Src clone with Y418). Recombinant protein A and PTK inhibitors (genistein, erbstatin analogue, herbimycin A, PP1, PP2) as well as control drugs (daidzein, PP3) were from Calbiochem. Stock solutions of PTK inhibitors were prepared in DMSO. Cytochalasin B and the myosin ATPase inhibitor BDM were from Sigma-Aldrich.

Bead preparation and bead assays

Silica beads (5 μm in diameter, with aminopropyl functional groups; Bangs Laboratories, Inc.) for RBIs were coated with either purified apCAM, 4E8 antibody, or Con A as described previously (Thompson et al., 1996; Suter et al., 1998). 4E8 was also directly (without protein A linkage) coupled to beads in order to reduce the level of bead labeling when 4E8 RBIs were followed by immunostaining with rabbit antibodies (Fig. 9). The RBI assay was performed as reported (Suter et al., 1998). 500-nm silica beads (Bangs Laboratories) were coated with Con A (Suter et al., 1998) or polyethylenimine (Forscher et al., 1992) and placed on the growth cone peripheral domain with an infrared single beam gradient laser trap to measure retrograde F-actin flow rates (Lin and Forscher, 1995).

Western blotting

The CNS tissue collected from two adult *Aplysia* was cut into small pieces and equally divided in lysis buffer (20 mM Hepes, pH 7.5, 150 mM NaCl, 1 mM EGTA, 1% Triton X-100, 0.5 mM Pefabloc (Boehringer), and 1% protease inhibitor cocktail (Sigma-Aldrich) substituted with and without phosphatase inhibitors (1 mM Na_3VO_4, 1 mM NaF), with and without 20 μM PP1, respectively. After incubation for 20 min on ice, the tissue was homogenized and cleared by centrifugation at 10,000 *g* for 20 min at 4°C. The protein concentration of the supernatant was determined with the BCA assay (Pierce Chemical Co.) and 20 μg of protein was loaded per lane of a 10% SDS-PAGE. After transfer onto nitrocellulose, proteins were probed with anti-Src PY418 at 0.5 μg/ml. Detection was performed with the ECL method according to the manufacturer's instructions (Amersham Pharmacia Biotech). After stripping the membrane with 100 mM 2-mercaptoethanol, 2% SDS, 62.5 mM Tris-HCl, pH 6.7, at 50°C for 30 min and washing with TBS/0.1% Tween, reprobing was performed with a monoclonal anti-β tubulin antibody (Sigma-Aldrich) at 1:10,000. For quantification, densitometry of blots was done with the 1D gel analysis tool of Metamorph 4.0 (Universal Imaging Corp.), and amounts of activated Src PTK were normalized against tubulin for equal protein loading.

Cell culture

Aplysia bag cell neurons were cultured on polylysine-coated coverslips in L15 medium (Life Technologies) supplemented with artificial seawater as described previously (Forscher and Smith, 1988; Suter et al., 1998). During experiments involving application of beads, the medium was supplemented with 5 mg/ml BSA to block nonspecific bead binding.

Video light microscopy and image processing

Video-enhanced differential interference contrast (DIC) time-lapse and fluorescence microscopy were performed as described (Forscher and Smith, 1988; Lin and Forscher, 1993, 1995; Suter et al., 1998). A 151-AT series image processor (Imaging Technology, Inc.) was used for real time video image processing, image analysis using custom-written software, and image digitization for export into Adobe Photoshop® 4.0 for image processing. The fluorescence images of Figs. 8 and 9 were taken with a Photometrics CoolSNAP Fx cooled CCD camera (Roper Scientific). Metamorph 4.0 was used for making montages of time-lapse sequences and image analysis. Confocal images were from an MRC-1024 microscope (Bio-Rad Laboratories).

PTK inhibitor experiments

In all experiments involving inhibitors, a red long pass filter (590 nm cut on) was used for DIC time-lapse recording. Bag cell growth cones were observed first under control conditions (medium plus DMSO), then treated

for 20 min with inhibitors. During this period exposure to light was kept to a minimum to avoid potential phototoxic effects. The same experimental paradigm was used to assess PTK inhibitor effects in the RBI assay. Only growth cones that had successfully interacted with the bead under control conditions were treated with the drug for 20 min and then reassessed for RBI capability. Beads were restrained in the presence of PTK inhibitors for at least 15 min, which exceeds the average latency time for control RBIs by >50% (latency period is operationally defined as the interval between bead placement and observable advance of the central cytoplasmic domain; Suter et al., 1998). In most experiments, RBI capability was also reassessed after drug removal.

Fluorescence labeling

Bag cell neurons were fixed by rapid exchange of the medium with 3.7% formaldehyde in artificial seawater supplemented with 400 mM sucrose. After fixation for 30 min, the cells were permeabilized for 10 min using 0.1% saponin (Sigma-Aldrich) in the fixation solution. Cells were then washed three times with PBS containing 0.01% saponin (wash solution). For F-actin double labeling, Alexa 568 phalloidin (Molecular Probes) was incubated at 1 U/ml in wash solution for 15 min. After three washes, the cells were blocked with 5% BSA (plus 10% goat serum; Sigma-Aldrich) in the case of Src PY418 labeling) in wash solution for 30 min and incubated with the PY antibody 4G10 or the Src PY418 antibody at 5 μg/ml in blocking solution for 1 h at RT. After three washes, secondary antibodies conjugated to either Alexa 488 or Alexa 568 (Molecular Probes) were added at 20 μg/ml in blocking solution for 30 min at room temperature. The final wash solution was replaced with antifading solution (20 mM n-propyl-gallate [Sigma-Aldrich] in 80% glycerol/20% PBS, pH 8.5) before fluorescence inspection. In controls using secondary antibody alone no fluorescence signal could be detected. F-actin and microtubule double-labeling was performed as described previously (Lin and Forscher, 1993).

Quantification of PY immunostainings

Fluorescence intensity of digitized images was analyzed using the 151-AT image processor and custom written line scan and area intensity measurement software. To quantify PY intensity in peripheral domains, leading edge, and filopodia tips, 8–10 area intensity samples were taken per growth cone and then averaged and corrected for background. To determine the PY accumulation factor of bead–growth cone interaction sites, the average PY fluorescence intensity in 3 μm^2 areas distributed over the bead interaction sites was obtained. After background subtraction, this value was normalized against the average PY fluorescence intensity of the peripheral domain surrounding the interaction site. Average accumulation factors were determined from $n = 3$–4 experiments. The same analysis was performed for Src PY418 labeling using Metamorph 4.0 region tools.

Online supplemental material

Experiments shown in Fig. 2, C–E and in Fig. 6, E–G are viewable as QuickTime videos. Video 1: DIC time-lapse (50×) video of Con A RBI, followed by fixation and PY labeling. Video 2: DIC time-lapse (100×) video of 4E8 RBI in control condition. After release of the needle, bead moves with retrograde flow. Video 3: DIC time-lapse (100×) video of the same growth cone shown in Video 2, but in the presence of 25 μM PP1, which blocks the RBI. Note, growth cone morphology and dynamics are not affected by the drug, and the bead moves backward with retrograde flow after release of the needle restraint. Video 4: DIC time-lapse (100×) video of a 4E8 RBI on the same growth cone after drug washout. Videos are available at http://www.jcb.org/cgi/content/full/jcb.200107063/DC1.

The authors thank D. Kemler for help with Western blot experiments, the Kandel lab for 4E8 hybridomas, and Drs. H. Keshishian, M. Mooseker, T. Osterwalder, and A. Schaefer for valuable comments on the manuscript.

This work was supported by a National Institutes of Health grant RO1-NS28695 to P. Forscher and a postdoctoral fellowship from the Swiss National Science Foundation to D.M. Suter.

Submitted: 13 July 2001
Revised: 18 September 2001
Accepted: 21 September 2001

References

Akiyama, T., J. Ishida, S. Nakagawa, H. Ogawara, S. Watanabe, N. Itoh, M. Shibuya, and Y. Fukami. 1987. Genistein, a specific inhibitor of tyrosine-specific protein kinases. *J. Biol. Chem.* 262:5592–5595.

Atashi, J.R., S.G. Klinz, C.A. Ingraham, W.T. Matten, M. Schachner, and P.F. Maness. 1992. Neural cell adhesion molecules modulate tyrosine phosphorylation of tubulin in nerve growth cone membranes. *Neuron.* 8:831–842.

Beggs, H.E., P. Soriano, and P.F. Maness. 1994. NCAM-dependent neurite outgrowth is inhibited in neurons from Fyn-minus mice. *J. Cell Biol.* 127:825–833.

Beggs, H.E., S.C. Baragona, J.J. Hemperly, and P.F. Maness. 1997. NCAM140 interacts with the focal adhesion kinase p125(fak) and the SRC-related tyrosine kinase p59(fyn). *J. Biol. Chem.* 272:8310–8319.

Bray, D. 1984. Axonal growth in response to experimentally applied mechanical tension. *Dev. Biol.* 102:379–389.

Burden-Gulley, S.M., and V. Lemmon. 1996. L1, N-cadherin, and laminin induce distinct distribution patterns of cytoskeletal elements in growth cones. *Cell Motil. Cytoskeleton.* 35:1–23.

Burridge, K., and M. Chrzanowska-Wodnicka. 1996. Focal adhesions, contractility, and signaling. *Annu. Rev. Cell. Dev. Biol.* 12:463–518.

Cavallaro, U., J. Niedermeyer, M. Fuxa, and G. Christofori. 2001. N-CAM modulates tumour-cell adhesion to matrix by inducing FGF-receptor signalling. *Nat. Cell Biol.* 3:650–657.

Choquet, D., D.P. Felsenfeld, and M.P. Sheetz. 1997. Extracellular matrix rigidity causes strengthening of integrin- cytoskeleton linkages. *Cell.* 88:39–48.

Chrzanowska-Wodnicka, M., and K. Burridge. 1996. Rho-stimulated contractility drives the formation of stress fibers and focal adhesions. *J. Cell Biol.* 133: 1403–1415.

Desai, C.J., Q. Sun, and K. Zinn. 1997. Tyrosine phosphorylation and axon guidance: of mice and flies. *Curr. Opin. Neurobiol.* 7:70–74.

Doherty, P., and F.S. Walsh. 1996. CAM-FGF receptor interactions: a model for axonal growth. *Mol. Cell. Neurosci.* 8:99–111.

Faivre-Sarrailh, C., J. Falk, E. Pollerberg, M. Schachner, and G. Rougon. 1999. NrCAM, cerebellar granule cell receptor for the neuronal adhesion molecule F3, displays an actin-dependent mobility in growth cones. *J. Cell Sci.* 112: 3015–3027.

Felsenfeld, D.P., P.L. Schwartzberg, A. Venegas, R. Tse, and M.P. Sheetz. 1999. Selective regulation of integrin–cytoskeleton interactions by the tyrosine kinase Src. *Nat. Cell Biol.* 1:200–206.

Forscher, P., and S.J. Smith. 1988. Actions of cytochalasins on the organization of actin filaments and microtubules in a neuronal growth cone. *J. Cell Biol.* 107:1505–1516.

Forscher, P., C.H. Lin, and C. Thompson. 1992. Novel form of growth cone motility involving site-directed actin filament assembly. *Nature.* 357:515–518.

Glogauer, M., P. Arora, G. Yao, I. Sokholov, J. Ferrier, and C.A. McCulloch. 1997. Calcium ions and tyrosine phosphorylation interact coordinately with actin to regulate cytoprotective responses to stretching. *J. Cell Sci.* 110:11–21.

Goldberg, D.J., and D.Y. Wu. 1996. Tyrosine phosphorylation and protrusive structures of the growth cone. *Perspect. Dev. Neurobiol.* 4:183–192.

Goodman, C.S. 1996. Mechanisms and molecules that control growth cone guidance. *Annu. Rev. Neurosci.* 19:341–377.

Hanke, J.H., J.P. Gardner, R.L. Dow, P.S. Changelian, W.H. Brissette, E.J. Weringer, B.A. Pollok, and P.A. Connelly. 1996. Discovery of a novel, potent, and Src family-selective tyrosine kinase inhibitor. Study of Lck- and FynT-dependent T cell activation. *J. Biol. Chem.* 271:695–701.

Helmke, S., and K.H. Pfenninger. 1995. Growth cone enrichment and cytoskeletal association of non-receptor tyrosine kinases. *Cell. Motil. Cytoskeleton.* 30: 194–207.

Ignelzi, M.A., Jr., D.R. Miller, P. Soriano, and P.F. Maness. 1994. Impaired neurite outgrowth of src-minus cerebellar neurons on the cell adhesion molecule L1. *Neuron.* 12:873–884.

Katz, B.Z., E. Zamir, A. Bershadsky, Z. Kam, K.M. Yamada, and B. Geiger. 2000. Physical state of the extracellular matrix regulates the structure and molecular composition of cell-matrix adhesions. *Mol. Biol. Cell.* 11:1047–1060.

Keller, F., and S. Schacher. 1990. Neuron-specific membrane glycoproteins promoting neurite fasciculation in *Aplysia* californica. *J. Cell Biol.* 111:2637–2650.

Kunz, S., U. Ziegler, B. Kunz, and P. Sonderegger. 1996. Intracellular signaling is changed after clustering of the neural cell adhesion molecules axonin-1 and NgCAM during neurite fasciculation. *J. Cell Biol.* 135:253–267.

Lamoureux, P., R.E. Buxbaum, and S.R. Heidemann. 1989. Direct evidence that growth cones pull. *Nature.* 340:159–162.

Lin, C.H., and P. Forscher. 1993. Cytoskeletal remodeling during growth cone-target interactions. *J. Cell Biol.* 121:1369–1383.

Lin, C.H., C.A. Thompson, and P. Forscher. 1994. Cytoskeletal reorganization underlying growth cone motility. *Curr. Opin. Neurobiol.* 4:640–647.

Lin, C.H., and P. Forscher. 1995. Growth cone advance is inversely proportional to retrograde F-actin flow. *Neuron.* 14:763–771.

Lin, C.H., E.M. Espreafico, M.S. Mooseker, and P. Forscher. 1996. Myosin drives

retrograde F-actin flow in neuronal growth cones. *Neuron.* 16:769–782.

Mallavarapu, A., and T. Mitchison. 1999. Regulated actin cytoskeleton assembly at filopodium tips controls their extension and retraction. *J. Cell Biol.* 146: 1097–1106.

Maness, P.F., M. Aubry, C.G. Shores, L. Frame, and K.H. Pfenninger. 1988. c-src gene product in developing rat brain is enriched in nerve growth cone membranes. *Proc. Natl. Acad. Sci. USA.* 85:5001–5005.

Maness, P.F., H.E. Beggs, S.G. Klinz, and W.R. Morse. 1996. Selective neural cell adhesion molecule signaling by Src family tyrosine kinases and tyrosine phosphatases. *Perspect. Dev. Neurobiol.* 4:169–181.

Matten, W.T., M. Aubry, J. West, and P.F. Maness. 1990. Tubulin is phosphorylated at tyrosine by pp60c-src in nerve growth cone membranes. *J. Cell Biol.* 111:1959–1970.

Mayford, M., A. Barzilai, F. Keller, S. Schacher, and E.R. Kandel. 1992. Modulation of an NCAM-related adhesion molecule with long-term synaptic plasticity in *Aplysia*. *Science.* 256:638–644.

Menon, K.P., and K. Zinn. 1998. Tyrosine kinase inhibition produces specific alterations in axon guidance in the grasshopper embryo. *Development.* 125: 4121–4131.

Mitchison, T., and M. Kirschner. 1988. Cytoskeletal dynamics and nerve growth. *Neuron.* 1:761–772.

Mohamed, A.S., K.A. Rivas-Plata, J.R. Kraas, S.M. Saleh, and S.L. Swope. 2001. Src-class kinases act within the agrin/MuSK pathway to regulate acetylcholine receptor phosphorylation, cytoskeletal anchoring, and clustering. *J. Neurosci.* 21:3806–3818.

Morse, W.R., J.G. Whitesides, A.S. LaMantia, and P.F. Maness. 1998. p59fyn and pp60c-src modulate axonal guidance in the developing mouse olfactory pathway. *J. Neurobiol.* 36:53–63.

Orioli, D., M. Henkemeyer, G. Lemke, R. Klein, and T. Pawson. 1996. Sek4 and Nuk receptors cooperate in guidance of commissural axons and in palate formation. *EMBO J.* 15:6035–6049.

Pelham, R.J., Jr., and Y. Wang. 1997. Cell locomotion and focal adhesions are regulated by substrate flexibility. *Proc. Natl. Acad. Sci. USA.* 94:13661–13665.

Riveline, D., E. Zamir, N.Q. Balaban, U.S. Schwarz, T. Ishizaki, S. Narumiya, Z. Kam, B. Geiger, and A.D. Bershadsky. 2001. Focal contacts as mechanosensors: externally applied local mechanical force induces growth of focal contacts by an mDia1-dependent and ROCK-independent mechanism. *J. Cell Biol*. 153:1175–1186.

Rochlin, M.W., M.E. Dailey, and P.C. Bridgman. 1999. Polymerizing microtubules activate site-directed F-actin assembly in nerve growth cones. *Mol. Biol. Cell.* 10:2309–2327.

Saffell, J.L., E.J. Williams, I.J. Mason, F.S. Walsh, and P. Doherty. 1997. Expression of a dominant negative FGF receptor inhibits axonal growth and FGF receptor phosphorylation stimulated by CAMs. *Neuron.* 18:231–242.

Sanna, P.P., F. Berton, M. Cammalleri, M.K. Tallent, G.R. Siggins, F.E. Bloom, and W. Francesconi. 2000. A role for Src kinase in spontaneous epileptiform activity in the CA3 region of the hippocampus. *Proc. Natl. Acad. Sci. USA.* 97:8653–8657.

Schaefer, A.W., H. Kamiguchi, E.V. Wong, C.M. Beach, G. Landreth, and V. Lemmon. 1999. Activation of the MAPK signal cascade by the neural cell adhesion molecule L1 requires L1 internalization. *J. Biol. Chem.* 274: 37965–37973.

Schmid, R.S., W.M. Pruitt, and P.F. Maness. 2000. A MAP kinase-signaling pathway mediates neurite outgrowth on L1 and requires Src-dependent endocytosis. *J. Neurosci.* 20:4177–4188.

Schmidt, C., H. Pommerenke, F. Durr, B. Nebe, and J. Rychly. 1998. Mechanical stressing of integrin receptors induces enhanced tyrosine phosphorylation of cytoskeletally anchored proteins. *J. Biol. Chem.* 273:5081–5085.

Schoenwaelder, S.M., and K. Burridge. 1999. Bidirectional signaling between the cytoskeleton and integrins. *Curr. Opin. Cell Biol.* 11:274–286.

Sicheri, F., and J. Kuriyan. 1997. Structures of Src-family tyrosine kinases. *Curr. Opin. Struct. Biol.* 7:777–785.

Suter, D.M., L.D. Errante, V. Belotserkovsky, and P. Forscher. 1998. The Ig superfamily cell adhesion molecule, apCAM, mediates growth cone steering by substrate-cytoskeletal coupling. *J. Cell Biol.* 141:227–240.

Suter, D.M., and P. Forscher. 1998. An emerging link between cytoskeletal dynamics and cell adhesion molecules in growth cone guidance. *Curr. Opin. Neurobiol.* 8:106–116.

Tanaka, E., and J. Sabry. 1995. Making the connection: cytoskeletal rearrangements during growth cone guidance. *Cell.* 83:171–176.

Tessier-Lavigne, M., and C.S. Goodman. 1996. The molecular biology of axon guidance. *Science.* 274:1123–1133.

Thomas, S.M., and J.S. Brugge. 1997. Cellular functions regulated by Src family kinases. *Annu. Rev. Cell. Dev. Biol.* 13:513–609.

Thompson, C., C.H. Lin, and P. Forscher. 1996. An *Aplysia* cell adhesion molecule associated with site-directed actin filament assembly in neuronal growth cones. *J. Cell Sci*. 109:2843–2854.

Walsh, F.S., and P. Doherty. 1997. Neural cell adhesion molecules of the immunoglobulin superfamily: role in axon growth and guidance. *Annu. Rev. Cell. Dev. Biol.* 13:425–456.

Wang, N., J.P. Butler, and D.E. Ingber. 1993. Mechanotransduction across the cell surface and through the cytoskeleton. *Science.* 260:1124–1127.

Williams, E.J., F.S. Walsh, and P. Doherty. 1994. Tyrosine kinase inhibitors can differentially inhibit integrin-dependent and CAM-stimulated neurite outgrowth. *J. Cell Biol.* 124:1029–1037.

Wills, Z., J. Bateman, C.A. Korey, A. Comer, and D. Van Vactor. 1999. The tyrosine kinase Abl and its substrate enabled collaborate with the receptor phosphatase Dlar to control motor axon guidance. *Neuron.* 22:301–312.

Worley, T., and C. Holt. 1996. Inhibition of protein tyrosine kinases impairs axon extension in the embryonic optic tract. *J. Neurosci.* 16:2294–2306.

Wu, D.Y., and D.J. Goldberg. 1993. Regulated tyrosine phosphorylation at the tips of growth cone filopodia. *J. Cell Biol.* 123:653–664.